CHAPTER EIGHTEEN

Probing Nucleic Acid–Ion Interactions with Buffer Exchange-Atomic Emission Spectroscopy

Max Greenfeld* *and* Daniel Herschlag†

Contents

Abstract

The ion atmosphere of nucleic acids directly affects measured biochemical and biophysical properties. However, study of the ion atmosphere is difficult due to its diffuse and dynamic nature. Standard techniques available have significant limitations in sensitivity, specificity, and directness of the assays. Buffer exchange-atomic emission spectroscopy (BE-AES) was developed to overcome many of the limitations of previously available techniques. This technique can provide a complete accounting of all ions constituting the ionic atmosphere of a nucleic acid at thermodynamic equilibrium. Although initially developed for the study of the ion atmosphere of nucleic acids, BE-AES has also been applied to study site-bound ions in RNA and protein.

1. Introduction

RNA folding and catalysis requires nonspecifically associated cations and often specifically bound ions for function. Specificity and affinity of DNA-binding proteins has been shown to be affected by ions in solution.

* Department of Chemical Engineering and Biochemistry, Stanford University, Stanford, California, USA
† Departments of Biochemistry and Chemistry, Stanford University, Stanford, California, USA

Methods in Enzymology, Volume 469
ISSN 0076-6879, DOI: 10.1016/S0076-6879(09)69018-2

Higher order assemblies including the ribosome and chromatin also depend on counterions (Herrera *et al.*, 1996; Tremethick, 2007). This strong functional dependence on counterions arises from the fact that RNA and DNA are polyelectrolytes with each residue having a formal negative charge. This results in a sheath of nonspecifically associated ions, called the ion atmosphere, forming around nucleic acids in solution (Draper, 2004; Manning, 1969a; Sharp and Hongin, 1995). For instance, in the absence of counterions the *Tetrahymena* Group I Intron would need to overcome a repulsion of 10^3 kcal/mol to fold into its active conformation (Bai *et al.*, 2005). The ion atmosphere greatly mitigates this repulsive force, although exact quantification remains difficult.

Extensive study has established that the ion atmosphere is a diffuse and dynamic structure (Misra and Draper, 2000) that cannot be described by simple ion-binding models (Manning, 1969a,b,c). This means that structural techniques such as crystallography or chemical footprinting cannot be used to study the ion atmosphere. Therefore, the techniques available for studying the ion atmosphere are severely restricted.

Line broadening in NMR spectra has been used to study $^{23}Na^+$ association with DNA. However, no rigorous relationship exists between line broadening and Na^+/DNA interactions, and the method is limited by available isotopes (Anderson and Record, 1990). Gel electrophoresis measures changes in the mobility of nucleic acids as affected by the presence of bulk ions, yet no formal relationship exists between mobility and the composition of the ion atmosphere (Li *et al.*, 1998). Anomalous small-angle X-ray scattering provides unique insight to the spatial distribution of ions in the ion atmosphere, but it does not directly count the number of ions in the atmosphere and is applicable for only select ions (Das *et al.*, 2003). Equilibrium dialysis read out by atomic absorption spectroscopy is an elegant approach for assaying the ion atmosphere. However, the original implementation for measuring Mg^{2+} association with tRNA was hindered in accuracy and throughput (Bina-Stein and Stein, 1976; Stein and Crothers, 1976a,b). Perhaps, the most extensively used technique involves fluorescent indicator dyes to assay the concentration of ions in solution. In practice, this technique only allows monitoring of a few select divalent ions, and as such has not been able to provide a complete accounting of the ion atmosphere (Grilley *et al.*, 2009; Krakauer, 1971; Romer and Hach, 1975). Nevertheless, this technique has proven an informative approach for studying the effect of the ion atmosphere on the energetics of tertiary structure formation in RNA (Grilley *et al.*, 2006, 2007).

To overcome the limitations of other techniques, buffer exchange-atomic emission spectroscopy (BE-AES) was created (Bai *et al.*, 2007). Measurements of the ion atmosphere done with BE-AES provide a rigorous thermodynamic measure of the number of ions associated with a nucleic acid. BE-AES is sensitive to a wide number of elements and has proven to

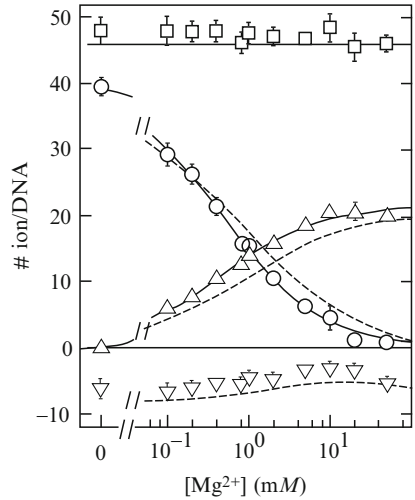

Figure 18.1 Competitive association between Mg^{2+} (Δ) and 20 (mM) Na^{+} (○) with a 24 bp DNA duplex. Depleted anions are shown by (▽) and the net charge is given by (□). Solid lines are fitted to the Hill equation (Eq. (18.3)), while dotted lines are predictions from the nonlinear Poisson–Boltzman model. Reprinted from Bai *et al.* (2007).

be highly sensitive and accurate. BE-AES was used to provide the first rigorous experimental evidence that ion size, a parameter not included in the widely used nonlinear Poisson–Boltzmann electrostatic theory, affects the occupancy of the ion atmosphere (Bai *et al.*, 2007). BE-AES has also been used to test for site-specific ion binding in RNA and protein model systems (Das *et al.*, 2005; Zalatan *et al.*, 2008).

Figure 18.1 indicates the type of data that can be gathered from a typical BE-AES experiment (Bai *et al.*, 2007). In this experiment the ions associated with a 24-bp DNA duplex (net charge +46) were measured for a series of Mg^{2+} concentrations. As expected, Mg^{2+} displaces Na^{+} with increased Mg^{2+} concentration. At the same time, the net charge on the system remains neutral. This chapter details the general and technical principles necessary for performing experiments analogous to those shown in Fig. 18.1. In addition, a detailed protocol for the experiments shown in Fig. 18.1 is presented.

2. Description of BE-AES

Key to studying the thermodynamics of nucleic acid ion association is establishing an equilibrium with a well-defined reference solution. BE-AES accomplishes this through the use of ultrafiltration spin columns that allow multiple buffer exchanges to be completed on one sample without

significant loss of sample. This approach achieves equilibrium much faster than standard equilibrium dialysis. Once equilibrium is reached, the number of ions associated with a nucleic acid is simply the enrichment of ion concentration, over the reference buffer, normalized by the concentration of macromolecules. Equation (18.1) formally shows this relationship:

$$N_{\#\mathrm{ion/na}} = \frac{c_{\mathrm{ion}}^{\mathrm{na}} - c_{\mathrm{ion}}^{\mathrm{buffer}}}{c_{\mathrm{na}}} \tag{18.1}$$

$c_{\mathrm{ion}}^{\mathrm{na}}$ indicates the concentration of the ionic atmosphere species in the nucleic acid containing sample, $c_{\mathrm{ion}}^{\mathrm{buffer}}$ indicates the concentration of the ionic atmosphere species in the reference buffer, and c_{na} indicates the concentration of nucleic acid (i.e., determined as the phosphorus concentration divided by the number of formal negative charges on the nucleic acid) in the nucleic acid containing sample. Experimental realization of the relationship outlined in Eq. (18.1) has been historically limited by the techniques available for determining ion concentrations. This limitation has been largely overcome through the application of modern inductively coupled plasma atomic emission spectroscopy (ICP-AES) for the determinations of the concentrations in Eq. (18.1). The advantages afforded by ICP-AES are twofold: (1) simultaneous quantification of multiple elements and (2) high accuracy over a broad range of ion concentrations. The simultaneous concentration determination of multiple ions in the ion atmosphere (e.g., sodium and magnesium) in addition to phosphorous (i.e., the nucleic acid) allows internally calibrated measurements that greatly increases the accuracy of BE-AES experiments.

Figure 18.2 diagrams the workflow of a typical BE-AES experiment. There are two major experimental steps: (1) buffer equilibration and (2) ICP-AES concentration determination. Both sample preparation (i.e., buffer exchange) and sample concentration determination (i.e., AES) must be successfully completed in order to make meaningful measurements. To maximize the utility of BE-AES, experimental design must carefully balance practical issues such as the availability and behavior of the nucleic acid being studied with the desire to get high precision and accuracy in the final measurements.

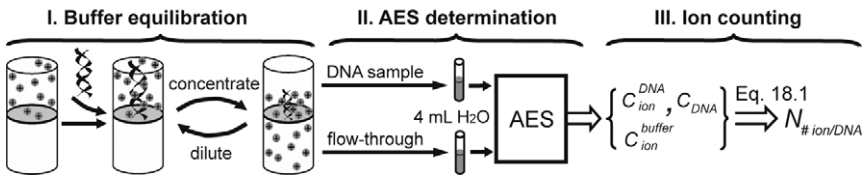

Figure 18.2 Schematic depicting the three major steps of BE-AES. Reprinted from Bai *et al.* (2007).

3. Buffer Equilibration

As depicted in Fig. 18.2, the first step in BE-AES is sequential buffer exchanges using ultrafiltration spin columns. Buffer exchanges are necessary to get the analyte into a known reference buffer. The last round of buffer exchange is used to concentrate the sample.

The accuracy of BE-AES measurements is directly related to the accuracy with which a solution concentration can be determined. ICP-AES, requires milliliter quantities of sample to accurately determine a concentration. However, the technique is sensitive to low micromolar concentrations of most elements. The high analyte concentrations obtained during the final concentrating step are necessary for maximizing the difference in concentrations between the two buffer chambers and as such must be diluted prior to ICP-AES concentration determination. Table 18.1 indicates approximate concentrations and volumes present during buffer equilibration and ICP-AES concentration determination. Unless otherwise noted, concentrations are the actual concentration in the buffer equilibrium step prior to dilution for ICP-AES measurement.

For any particular ion being studied, Eq. (18.1) indicates three concentrations that must be determined. However, the difference in concentration between $c_{\mathrm{ion}}^{\mathrm{na}}$ and $c_{\mathrm{ion}}^{\mathrm{buffer}}$ must be sufficiently large that it can be determined with accuracy comparable to c_{na}. The value of $c_{\mathrm{ion}}^{\mathrm{buffer}}$ can be determined with the highest precision because there is a large quantity of this material which can be measured. In practice, the analyte must be concentrated to a concentration of hundreds of micromolar to afford a sufficiently large differential in $c_{\mathrm{ion}}^{\mathrm{DNA}}$ and $c_{\mathrm{ion}}^{\mathrm{buffer}}$. At this concentration an amount of analyte of 20–40 μL is sufficient to accurately determine the concentration.

Although buffer exchanging and concentration is technically simple, careful experimental design is necessary for ensuring that meaningful results are obtained and to prevent the use of unnecessarily large quantities of a nucleic acid. There are tradeoffs between working at high concentrations of a nucleic acid, which ensures good signal, with the complications that arise

Table 18.1 Typical sample concentrations and volumes

	I. Buffer equilibration	II. AES determination
Concentration analyte	0.01–10 (m*M*)	0.01–20 (μM)
Volume	100 (μL)	4 (mL)

Actual concentration ranges of analyte in the buffer equilibration step and the AES concentration determination step. Unless otherwise noted concentrations listed in the text are the actual concentrations in the buffer equilibration step prior to dilution for AES measurements.

with working at high concentrations. BE-AES experiments must be designed such that the following criteria are met: (1) results are independent of the final macromolecule concentration; (2) equilibrium has been reached; and (3) analyte concentrations are stable between sample preparation and ICP-AES measurements.

The high final concentrations of an analyte can result in at least two problems. First, precipitation of nucleic acids can be a problem at high concentrations. The experimentalist should be vigilant during sample preparation to ensure that no signs of precipitation are observed. Second, interactions between nucleic acids can still occur without precipitation. This possibility necessitates controls where BE-AES results are shown to be the same over a range of nucleic acid concentrations.

Establishing that equilibrium has been reached is central to measuring any thermodynamic quantity. In BE-AES, equilibrium can be verified by measuring the composition of the flow-through buffer of a spin column. The flow-through buffer of a spin column should remain constant over sequential rounds of buffer exchanges and should be of identical composition to the buffer being used for buffer exchanges. Figure 18.3 shows the change in ion concentration of the flow-through for sequential rounds of buffer exchanges. The number of rounds of buffer exchange needed to reach equilibrium depends on the composition of the buffer being used.

The stability of the analyte concentrations can be disturbed by unintended sources. Two sources that have been identified are evaporation and

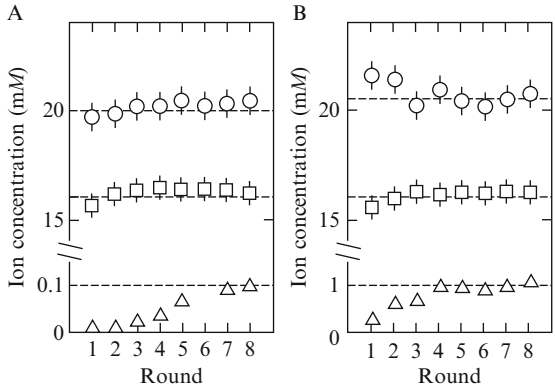

Figure 18.3 Ensuring equilibrium has been reached requires monitoring the concentration of the flow-through in sequential buffer exchanges. Plots depict the ion concentration in the flow-through for sequential rounds of buffer exchanges. (A) 0.1 m*M* Mg^{2+} (Δ), 20 m*M* Na^{+} (○), and 16 m*M* cacodylate (□). (B) 1 m*M* Mg^{2+} (Δ), 20 m*M* Na^{+} (○), and 16 m*M* cacodylate (□). A final concentration of 0.5 m*M* DNA was targeted. Note that at lower Mg^{2+} more rounds of buffer exchange were needed to achieve equilibrium. Reprinted from Bai *et al.* (2007).

nonspecific loss during ICP-AES analysis. It is prudent to design experiments and controls with these potential sources of error in mind since data obtained with solutions of poorer stability will not necessarily look wrong. Rather, the experimentalist might have undesirable irreproducibility of measurements or systematic error not consistent with a well-known property of the system, such as charge neutrality.

Evaporation can become a problem when small sample volumes are used for the final concentration of a sample. The large exposed surface area of spin columns and the time required for concentration are sufficient for evaporation to affect the final measured concentration. Figure 18.4 shows that some sample preparation protocols can result in up to a 15% error due to evaporation. In contrast, protocols designed to minimize evaporation can reduce error due to evaporation to negligible amounts. The easiest way to get around this problem is to use a large sample volume. Unfortunately, to maintain the same signal, large quantities of the nucleic acid being studied must be used for the buffer exchanges. This solution results in a large fraction of unanalyzed sample that can typically be recovered and used in subsequent experiments. Additionally, care can be taken to minimize evaporation, such as preparing samples in a cold room, or not letting them sit for a long time before the final dilution.

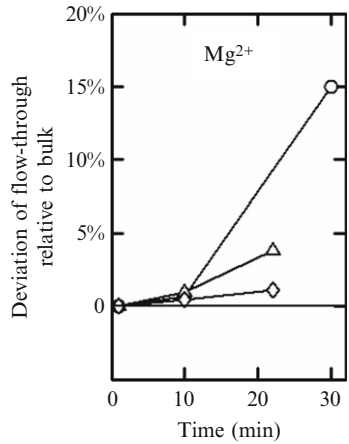

Figure 18.4 The time required for buffer exchanges can be sufficient for evaporation to affect the concentration of ions. Demonstration that the collected Mg^{2+} concentration can systematically increase with time. Flow-through was collected at 1, 10, and 20 or 30 min (corresponding to 450, 250, and 100 or 20 μL of solution remaining in the top chamber) during the final round of buffer equilibration. Deviations from the starting buffer concentration (1 m*M* Mg^{2+}, 20 m*M* Na^{+}, and 16 m*M* cacodylate) are plotted for equilibrium conditions that affect total evaporation. Buffer exchanges were carried out at 25 °C and retained volume of 20 μL (○), 25 °C and retained volume of 100 μL (Δ), and 4 °C and retained volume of 100 μL (◇). Reprinted from Bai *et al.* (2007).

The low concentrations of analyte in ICP-AES measurements can change significantly due to small nonspecific losses of sample through precipitation. This can potentially be dealt with by doing the final dilution of a sample immediately prior to ICP-AES analysis. This is a viable solution if the precipitation is not significant on the timescale of a few hours. Alternatively, it may be possible to stabilize the solution with different buffering conditions. Particularly relevant are low pH buffers, which can help prevent the formation of insoluble metal oxides. Verifying reproducibility with tubes made of different materials or made by different manufacturers is useful for verifying that erroneous results are not arising from nonspecific absorption to tubes or leaching of material from the tubes.

4. ICP-AES

ICP-AES is a highly sensitive technique for determining the atomic composition of solutions. As shown in Table 18.2, ICP-AES is able to simultaneously detect many biologically relevant elements. As biophysical studies will inevitably rely on sample dilution to arrive at the concentration

Table 18.2 Selected elements detectable with ICP-AES. Reprinted from Bai *et al.* (2007)

Element	Detection limit (n*M*)	Linear range[a] (m*M*)
Arsenic	100	0.01–2
Barium	1	0 1–0.5
Cadmium	5	ND
Calcium	150	0.01–0.5
Chloride[b]	ND	ND
Cobalt	50	ND
Lithium	300	0.1–2.5
Magnesium	80	0.0 1–0.5
Manganese	300	ND
Phosphorous	65	0.025–2
Potassium	250	0.1–2.5
Rubidium	ND	0.1–2.5
Sodium	300	0.2–2.5
Zinc	15	ND

[a] Linear regime was defined as the region for which the expected concentration deviated no more than 5% from the measured values.
[b] Detection of halides requires specialized detectors not available on many ICP-AES instruments.
ND indicates not determined.

of sample for ICP-AES analysis, the lower limit of detection is useful to keep in mind so as to avoid working at unnecessarily high concentrations that waste analyte. The 100–200-fold dilutions used for most measurements the authors have taken lie within the linear range reported in Table 18.2. The reported linear range was optimized for low concentrations of analyte. ICP-AES is capable of directly measuring higher concentrations, but this will sacrifice the accuracy of lower concentration measurements. If the details of a particular experiment allow for larger quantities of the analyte to be easily made, using a smaller dilution factor, which sacrifices the high sensitivity of ICP-AES, would likely yield more accurate results.

Often ICP-AES instruments are run by operators who are highly knowledgeable about the intricacies of their particular instrument. Discuss with the operator what samples you are running. They will probably have suggestions of how to set up a sample run to make things run quickly and most accurately. However, ICP-AES has many analytical uses, probably least of which are biophysical measurements. This is not a problem; however, it should be remembered that some of the advice from standard ICP-AES references does not transfer directly to use with biological macromolecules.

5. Measuring Anions

Most ICP-AES instruments are not equipped with a detector sensitive to Cl^- or other halides. To compensate for this limitation, cacodylate ($(CH_3)_2AsO_2^-$), or potentially another detectable anion, can be used as a proxy for the other anions. As shown in Eq. (18.2), the total number of excluded anions can be inferred from measuring the number of excluded cacodylate anions and scaling that number by the ratio of total anions to cacodylate

$$M_{\text{depleted}} = \text{AsO}_2(\text{CH}_3)_{2\,\text{depleted}}^- \frac{[\text{M}^-]}{[\text{AsO}_2(\text{CH}_3)_2^-]} \tag{18.2}$$

This relationship assumes that all anions behave in the same way. To have confidence that the cacodylate concentrations are reflective of the actual anions of interest, the two controls outlined in Fig. 18.5 need to be completed. As cacodylate has a pK_a of 6.3, it is necessary to make sure that the anion is the primary species present. As shown in Fig. 18.5A, this is done by verifying that the number of excluded anions does not vary as a function of the pH of the reference buffer. Additionally, as the size of the anion could affect how it is excluded, it is prudent to verify that the number of excluded anions does not change with the fractional abundance of the cacodylate. Figure 18.5B demonstrates that this assumption does hold for duplex DNA.

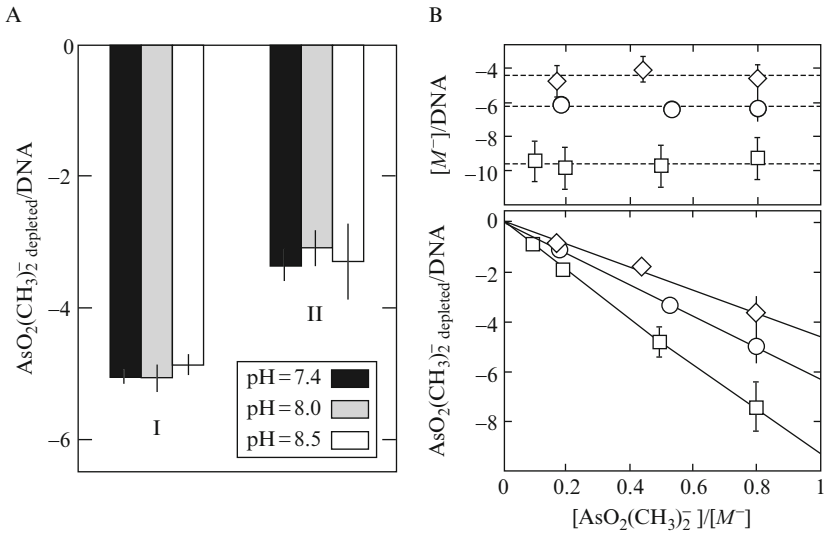

Figure 18.5 Most atomic anions are not detectable on common ICS-AES instruments. Addition of detectable anions can be used as proxies for more abundant anions. For a DNA duplex it was shown that cacodylate serves as a good substitute. (A) Excluded anions can be measured in a regime that is independent of pH for a 24-bp DNA duplex (I: 20 m*M* Na^+ with 10 m*M* cacodylate and II: 1 m*M* Mg^{2+} 20 m*M* Na^+ with 10 m*M* cacodylate). (B) The calculated number of excluded anions (see Eq. (18.2)) does not depend on the fractional abundance of cacodylate for three ionic conditions: (○) 20 m*M* Na^+, (□) 100 m*M* Na^+, and (◊) 1 m*M* Mg^{2+} and 20 m*M* Na^+. Lines are least-squares linear fits. Total excluded anions per DNA are calculated according to Eq. (18.2) and are plotted above the main plot with the same symbols. Reprinted from Bai *et al.* (2007).

6. Example Protocol

This section outlines in detail the specific steps used to carry out the measurements shown in Fig. 18.1. Table 18.3 indicates the suppliers of the reagents and equipment used in gathering the example data. Alternative vendors have also been included for potential future reference.

1. Complementary DNA oligos (GGTGACGAGTGAGCTACTGGGCGG and CCGCCCAGTAGCTCACTCGTCACC) were purchased from commercial vendors (Integrated DNA Technologies or PAN Facility at Stanford) and purified using ion-exchange HPLC (Dionex, DNAPac PA-100). Collected fractions were concentrated and desalted using C-18 cartridges (Waters, Sep-Pak). Quantification of oligos was done using UV absorbance at 260 nm.
2. Equimolar amounts of complementary strands were annealed in 20 m*M* Na-EPPS (sodium 4-(2-hydroxyethyl)piperazine-10-propanesulfonic

Table 18.3 Vendors for experimental consumables

Consumable	Vendor	Product description
ICP Standards	SPEXCertiPrep	Assurance™ Standards
	Sigma-Aldrich	TraceCERT™
	RICCA Chemical Company	ICP Standards
Spin Columns	Millipore	Microcon™ Centrifugal Filter Units
	Millipore	MF-Millipore™ "V" Series Membranes
	Pierce	Slide-A-Lyzer™ MINI Dialysis Units
Tubes	Fisherbrand	Polystrene 13 × 100 mm Round-Bottom
	Falcon	Polystrene 13 × 100 mm Round-Bottom
Reagents	Fisher	Trace Metal Acids
	Sigma-Aldrich	Trace Metal Acids
Glassware	Kimax	Pipets and Flasks
	Pyrex	

acid), pH 8.0. Purity was checked with Nondenaturing polyacrylamide gel electrophoresis of 1 μg of annealed DNA stained with StainsAll (Sigma-Aldrich) indicating that negligible quantities of free single-stranded DNA were present.

3. Reagents used for buffers and dilutions should be checked for purity using ICP-AES. It is also recommended to determine the concentration of buffers with ICP-AES, as this will lead to internally calibrated measurements.
4. Microcon YM-30 (Millipore) spin columns were used to carry out buffer exchanges with 1 m*M* Mg^{2+} (in a typical experiment, see Fig. 18.1, multiple Mg^{2+} concentrations would be chosen), 20 m*M* Na^{+}, 16 m*M* cacodylate, and 8 m*M* EPPS, pH 8.0 buffer. Buffer equilibration was conducted at 4 °C, during which time the volume of DNA containing sample retained in the top chamber did not fall below 100 μL. Between six and eight rounds of buffer exchange were needed to reach equilibrium. Verification of equilibrium was determined as shown in Fig. 18.3. For the last round of buffer equilibration, the last 80–100 μL of flow-through was collected and is most representative the bulk solution of the DNA-containing sample. Buffer exchanges were done at a relative centrifugal force (RCF) of 10,000×*g*. Used at three-quarters of the maximum RCF recommended by the manufacturer, good batches of these columns will quantitatively retain the DNA in the top chamber of the spin column.

5. Aliquots of 20–40 μL from the top of the spin column (i.e., DNA-containing samples) and the final flow-through were added to polystyrene tubes (Fisher Science) containing 4 mL of water. It has subsequently been determined that diluting the sample in ammonium acetate buffer, pH 5.2, is superior to water. Dilution factors were such that the final concentration of all ions in the analyte remained in the linear range of ICP-AES measurements.
6. ICP-AES was done using an IRIS Advantage 1000 radial ICAP Spectrometer (Thermo Jarrell Ash). A calibration standard solution was made using volumetric glassware typically containing 100 μM of each element being studied. The calibration standard was made from certified single atom reference standards (SPEXCertiPrep). Serial dilutions of this standard can be used to generate standard curves analogous to the one shown in Fig. 18.6. The standard curve shown in Fig. 18.6 is adjusted to the

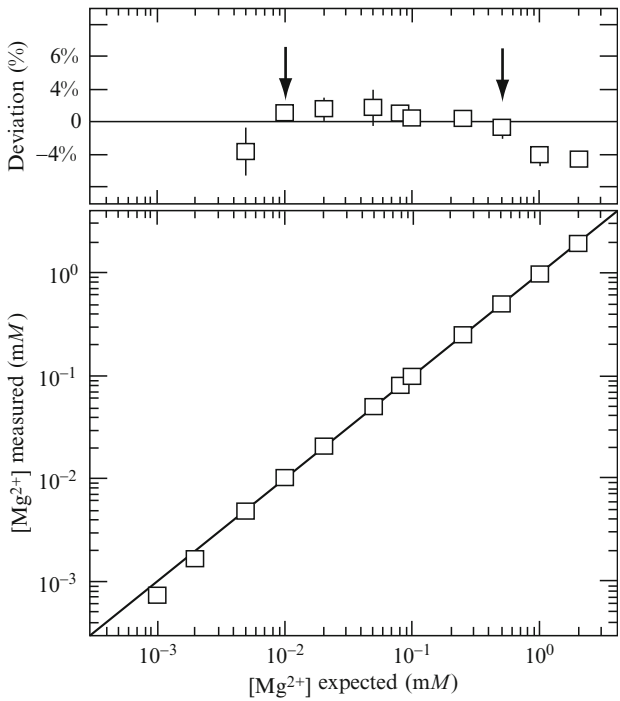

Figure 18.6 Representative standard curve of ICP-AES. Expected concentrations are based on reference standards of certified accuracy. The residual error of measured concentrations is plotted above the standard curve. Error bars represent standard errors of three or more replicate measurements. The linear concentration regime is bracketed by arrows and represents deviations of expected and measured concentrations of less than 5%. Reprinted from Bai *et al.* (2007).

concentrations present during buffer exchange before the 100–200× dilution necessary for ICP-AES.

Elements were monitored using the following atomic emission lines: As 189.042 nm, Mg 280.270 nm, Na 589.592 nm, P 213.618 nm. Prior to determining the concentration of each sample, the instrument was flushed with dilute nitric acid and then 1 mL of the analyte. The concentration of the remaining 3 mL of sample was determined three times sequentially. The average of the three measurements was used in the final analysis. However, spurious measurements among the three measurements can be an indication of a problem. The instrument was minimally programmed to measure a reference standard every 15 samples.

There is significant flexibility to the order in which samples are run on an ICP-AES. A good ICP-ASE can be stable enough that samples can be run in arbitrary order. However, it would be exceedingly difficult to diagnose problems if for any particular sample there was no expectation of what the concentration was. Table 18.4 indicates the typical order in which samples were run.

7. The data should be inspected for systematic error and spurious data points. If a large number of samples are being run, drift in the instrument calibration can cause deviations in the absolute concentration of elements measured. If this drift is uniform for all elements, the results will be minimally affected. However, differential drift among the elements being monitored is possible and will not have a benign effect. Spin column leakage or evaporation can often be detected by looking for

Table 18.4 Typical sample order for ICP-AES measurements

Sample number	Buffer	Description
1		0.1× calibration standard
2		0.2× calibration standard
3		0.5× calibration standard
4		0.8× calibration standard
5		1× calibration standard
6		Blank
7	1 m*M* Mg	Buffer no spin columns
8		Flow-through
9		Top
10	2 m*M* Mg	Buffer no spin columns
11		Flow-through
12		Top
13		etc.

Celebration standard: typically 100 μM of P, Mg, Na, and As.

spurious data points. Examples include phosphorus showing up in the flow-through, too little phosphorus being retained, and significantly higher concentrations of ions in the flow-through when compared to a reference sample. Any of these observations is an indication that one or more of the basic assumptions of BE-AES measurements is not met and are causes to reevaluate the procedure being carried out. It should be verified that the serial dilutions of the calibration have the expected values. If the deviations from a linear value are significant, a linear regime should be chosen and the concentrations recalibrated. Concentrations outside that range should not be used.

Once concentrations are determined, Eqs. (18.1) and (18.2) can be used to determine the individual components of the ion atmosphere. The effectiveness of one cation species out competing another cation was summarized in Fig. 18.1 by monitoring the number of competing cations (CC) and background cations (BC) associated with the DNA in accordance with Eq. (18.3). In Eq. (18.3) the *competition constant* was determined as the midpoint ($[M]_{1/2}$) of the BC association assuming a two state model:

$$N = N_1 + \frac{N_0 - N_1}{1 + ([M]/[M]_{1/2})^n} \tag{18.3}$$

where [M] is the titrated CC concentration and N_0 and N_1 are the number of BC at the start and end states. The Hill coefficient n is fitted simultaneously with $[M]_{1/2}$. The Hill analysis was carried out as an empirical description of the competition behavior and does not represent a physical model for ion binding (Das *et al.*, 2005; Draper, 2004).

ACKNOWLEDGMENTS

We are appreciative of technical assistance from Guangchao Li of the Stanford Geological and Environmental Sciences Department on ICP-AES measurements. We would like to thank Yu Bai for help in preparing the figures. Funding was provided by NIH program project grant P01-GM-66275 and an NIH grant GM49243 to D. H.

REFERENCES

Anderson, C. F., and Record, M. T. J. (1990). Ion distributions around DNA and other cylindrical polyions: Theoretical descriptions and physical implications. *Annu. Rev. Biophys. Biophys. Chem.* **19,** 423–465.

Bai, Y., Das, R., Millett, I., Herschlag, D., and Doniach, S. (2005). Probing counterion modulated repulsion and attraction between nucleic acid duplexes in solution. *Proc. Natl. Acad. Sci. USA* **102**(4), 1035–1040.

Bai, Y., Greenfeld, M., Travers, K. J., Chu, V. B., Lipfert, J., Doniach, S., and Herschlag, D. (2007). Quantitative and comprehensive decomposition of the ion atmosphere around nucleic acids. *J. Am. Chem. Soc.* **129**(48), 14981–14988.

Bina-Stein, M., and Stein, A. (1976). Allosteric interpretation of Mg^{2+} binding to the denaturable *Escherichia coli* tRNAGlu^{2+}. *Biochemistry* **15**(18), 3912–3917.

Das, R., Mills, T. T., Kwok, L. W., Maskel, G. S., Millett, I. S., Doniach, S., Finkelstein, K. D., Herschlag, D., and Pollack, L. (2003). Counterion distribution around DNA probed by solution X-ray scattering. *Phys. Rev. Lett.* **90**(18), 188103.

Das, R., Travers, K. J., Bai, Y., and Herschlag, D. (2005). Determining the Mg^{2+} stoichiometry for folding an RNA metal ion core. *J. Am. Chem. Soc.* **127**(23), 8272–8273.

Draper, D. (2004). A guide to ions and RNA structure. *RNA* **10**(3), 335–343.

Grilley, D., Soto, A. M., and Draper, D. E. (2006). Mg^{2+}-RNA interaction free energies and their relationship to the folding of RNA tertiary structures. *Proc. Natl. Acad. Sci. USA* **103**(38), 14003–14008.

Grilley, D., Misra, V., Caliskan, G., and Draper, D. E. (2007). Importance of partially unfolded conformations for Mg^{2+}-lnduced folding of RNA tertiary structure: Structural models and free energies of Mg^{2+} interactions. *Biochemistry* **46**(36), 10266–10278.

Grilley, D., Soto, A. M., and Draper, D. E. (2009). Direct quantitation of Mg^{2+}-RNA interactions by use of a fluorescent dye. *Methods Enzymol.* **455,** 71–94.

Herrera, J. E., Correia, J. J., Jones, A. E., and Olson, M. O. (1996). Sedimentation analyses of the salt- and divalent metal ion-induced oligomerization of nucleolar protein B23. *Biochemistry* **35**(8), 2668–2673.

Krakauer, H. (1971). The binding of Mg++ ions to polyadenylate, polyuridylate, and their complexes. *Biopolymers* **10**(12), 2459–2490.

Li, A. Z., Huang, H., Re, X., Qi, L. J., and Marx, K. A. (1998). A gel electrophoresis study of the competitive effects of monovalent counterion on the extent of divalent counterions binding to DNA. *Biophys. J.* **74**(2 Pt 1), 964–973.

Manning, G. (1969a). Limiting laws and counterion condensation in polyelectrolyte solutions I. Colligative properties. *J. Chem. Phys.* **51**(3), 924–933.

Manning, G. (1969b). Limiting laws and counterion condensation in polyelectrolyte solutions II. Self-diffusion of small ions. *J. Chem. Phys.* **51**(3), 934–938.

Manning, G. (1969c). Limiting laws and counterion condensation in polyelectrolyte solutions III. An analysis based on Mayer ionic solution theory. *J. Chem. Phys.* **51**(8), 3249–3252.

Misra, V., and Draper, D. (2000). Mg^{2+} binding to tRNA revisited: The nonlinear Poisson–Boltzmann model. *J. Mol. Biol.* **299**(3), 813–825.

Romer, R., and Hach, R. (1975). tRNA conformation and magnesium binding. A study of a yeast phenylalanine-specific tRNA by a fluorescent indicator and differential melting curves. *Eur. J. Biochem.* **55**(1), 271–284.

Sharp, K., and Hongin, B. (1995). Salt effects on nucleic-acids. *Curr. Opin. Struct. Biol.* **5**(3), 323–328.

Stein, A., and Crothers, D. M. (1976a). Equilibrium binding of magnesium(II) by *Escherichia coli* tRNAfMet. *Biochemistry* **15**(1), 157–160.

Stein, A., and Crothers, D. M. (1976b). Conformational changes of transfer RNA. The role of magnesium(II). *Biochemistry* **15**(1), 160–168.

Tremethick, D. J. (2007). Higher-order structures of chromatin: The elusive 30 nm fiber. *Cell* **128**(4), 651–654.

Zalatan, J. G., Fenn, T. D., and Herschlag, D. (2008). Comparative enzymology in the alkaline phosphatase superfamily to determine the catalytic role of an active-site metal ion. *J. Mol. Biol.* **384**(5), 1174–1189.